

## Magnetic structure of iron borate $\text{DyFe}_3(\text{BO}_3)_4$ : A neutron diffraction study

This content has been downloaded from IOPscience. Please scroll down to see the full text.

2012 J. Phys.: Conf. Ser. 340 012065

(<http://iopscience.iop.org/1742-6596/340/1/012065>)

View the [table of contents for this issue](#), or go to the [journal homepage](#) for more

Download details:

IP Address: 128.122.253.212

This content was downloaded on 21/10/2014 at 20:21

Please note that [terms and conditions apply](#).

## Magnetic structure of iron borate $\text{DyFe}_3(\text{BO}_3)_4$ : A neutron diffraction study

**C Ritter<sup>1</sup>, A Pankrats<sup>2</sup>, I Gudim<sup>2</sup> and A Vorotynov<sup>2</sup>**

<sup>1</sup> Institute Laue-Langevin, BP 156, F-38042 Grenoble, France

<sup>2</sup> L V Kirenskii Institute of Physics, Siberian Branch of RAS, Krasnoyarsk 660036, Russia

E-mail: ritter@ill.fr

**Abstract.** Neutron diffraction measurements were performed on the iron borate  $\text{DyFe}_3(\text{BO}_3)_4$  to investigate details of the crystallographic structure, the low temperature magnetic structure and its magnetic properties.  $\text{DyFe}_3(\text{BO}_3)_4$  adopts at room temperature the  $P3_121$  symmetry and becomes antiferromagnetic below  $T_N = 39$  K. Both, the rare earth and the iron sublattice, follow the same magnetic propagation vector  $\tau = [0, 0, \frac{1}{2}]$  which leads to a doubling of the crystallographic unit cell in the  $c$ -direction. The easy axis anisotropy of the rare earth determines the moment orientation to be mainly along  $c$ . No spin reorientation is found between  $T_N$  and 1.5 K, however, a small anomaly in the thermal dependence of the unit cell  $a$ -parameter is found at about 27 K which could be connected to repopulation of low lying Kramers doublets of  $\text{Dy}^{3+}$ . The magnetic moment value of the Fe-moment is at 1.5 K with  $\mu_{\text{Fe}} = 4.5 \mu_B$  only slightly smaller than expected for an  $S = 5/2$  ion while the Dy moment is strongly reduced and amounts only to  $\mu_{\text{Dy}} = 6.4 \mu_B$ .

### 1. Introduction

The family of rare earth ferroborates of general formula  $\text{RFe}_3(\text{BO}_3)_4$  where R is a rare earth or Y has recently attracted considerable attention due to their interesting magnetic, magnetoelectric and multiferroic properties [1-5]. The presence of two magnetic sublattices, a structure which sees helicoidal Fe-Fe-chains with a strong one-dimensional character and the absence of direct R-O-R-interactions [6] opens the way for a variety of magnetic ordering phenomena where the temperature dependent competition between the anisotropy of the rare earth sublattice and that of the iron sublattice leads to different magnetic structures and may induce spin reorientations and metamagnetic behavior. Previous neutron diffraction studies have established an easy-axis orientation of the magnetic moments for  $\text{R} = \text{Tb}, \text{Pr}$  [7, 8] over the whole temperature range below  $T_N$  and for  $\text{R} = \text{Ho}$  [9] below the spin reorientation temperature while for  $\text{R} = \text{Nd}, \text{Er}, \text{Ho}$  (above 5 K) and Y an easy-plane orientation has been found [10, 8, 9]. Magnetic resonance data indicate for  $\text{R} = \text{Gd}$  a spin reorientation from easy-plane to easy-axis on lowering the temperature [11]. Depending on the ionic size of the rare earth a structural transition from a high temperature  $R32$  phase to a low temperature  $P3_121$  phase can take place in the  $\text{RFe}_3(\text{BO}_3)_4$  compounds where the presence of two different iron sites can lead in the low symmetry  $P3_121$  phase to slightly different Fe-Fe distances along the

helicoidal chains and even to slightly different orientations of the two magnetic Fe sublattices [12, 13, 9]. The presence of short-range magnetic order within the helicoidal Fe-spin chains was determined to persist in  $\text{YFe}_3(\text{BO}_3)_4$  up to temperatures several times  $T_N$  adding a further piece to the highly interesting puzzle of the magnetic behavior of this family of compounds [14]. The second order antiferromagnetic transition leading to the long range ordered magnetic state seems to be driven by Fe-O-B-O-Fe superexchange interactions while the superexchange Fe-O-R-O-Fe pathway leads in all up to now known  $\text{RFe}_3(\text{BO}_3)_4$  compounds with magnetic R to  $T_{NR} = T_{NFe}$ .

Magnetization and specific heat data by Popova et al. [15] determined  $T_N = 38$  K for  $\text{DyFe}_3(\text{BO}_3)_4$  and qualified it as an easy-axis antiferromagnet. The authors of [15] described the magnetic behavior of the iron and the rare-earth sublattices as qualitatively different with the Dy-sublattice apparently staying paramagnetic down to lowest temperatures. Gudim et al [16] came from their magnetization data to the same conclusions as [15] concerning  $T_N$  and the easy-axis antiferromagnetic state of  $\text{DyFe}_3(\text{BO}_3)_4$ . Several groups [15-17] found a maximum in the magnetic susceptibility at about 25 K; this was explained [15, 17] to be caused by a repopulation of the two lowest  $\text{Dy}^{3+}$  energy levels. As part of a systematic study on the influence of the different rare earths on the magnetic behavior of  $\text{RFe}_3(\text{BO}_3)_4$  compounds we performed temperature dependent high resolution and high intensity neutron diffraction studies on  $\text{DyFe}_3(\text{BO}_3)_4$ .

## 2. Experimental details

### 2.1. Sample preparation

Single crystals of  $\text{DyFe}_3(\text{BO}_3)_4$  were prepared at the Institute of Physics at Krasnoyarsk following the preparation procedure described in detail in [16]. Because of the strong neutron absorption by natural boron 99% with  $^{11}\text{B}$  enriched  $\text{B}_2\text{O}_3$  was used. Powder samples were then made from the grown crystals.

### 2.2. Neutron diffraction measurements

Neutron diffraction data were taken at the Institut Laue-Langevin in Grenoble, France, using the high resolution powder diffractometer D2B ( $\lambda = 1.594$  Å) and the high flux powder diffractometer D20 ( $\lambda = 2.418$  Å). The sample was placed inside a thin vanadium container of 3 mm diameter in order to reduce the absorption from dysprosium. The temperature dependence was measured on D20 between 1.5 K and 50 K with a temperature resolution of about 0.6 K taking a spectrum every 10 min. High resolution data were taken on D2B at 1.5 K, 50 K and at room temperature. All data were refined by the Rietveld method using the FULLPROF [18] program.

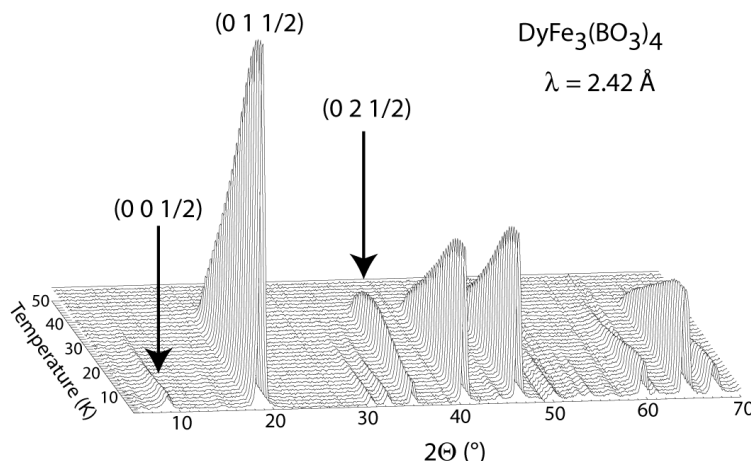


**Figure 1.** Thermal dependence of the magnetic scattering in  $\text{DyFe}_3(\text{BO}_3)_4$ .

### 3. Results and discussion

The high resolution neutron diffraction data taken at 300 K and 50 K (figure 2a) on D2B were used to refine the room temperature crystal structure and to verify the purity of the sample. No impurity phases are present and the fit proceeded smoothly in the spacegroup  $P3_121$ . Results of this refinement are shown in table 1 together with some selected interatomic distances. Error bars are slightly higher than usual due to the closeness of the structure to the higher symmetric phase  $R32$  which should be adopted by  $DyFe_3(BO_3)_4$  at about 340 K [12]. A fit of the 300 K data against the  $R32$  model resulted in significantly higher R-factors.

**Table 1.** Structural data at 1.5 K, 50 K and 300 K of  $DyFe_3(BO_3)_4$  refined in  $P3_121$  together with the most important interatomic distances.

$P3_121$	1.5 K	50 K	300 K
$a$ (Å)	9.5365(1)	9.5379(1)	9.5439(1)
$c$ (Å)	7.5621(1)	7.5609(1)	7.5676(1)
Dy (3a) $x$	0.3358(5)	0.3344(4)	0.3329(8)
Fe1 (3a) $x$	0.8825(7)	0.8829(6)	0.8850(10)
Fe2 (6c) $x$	0.7841(6)	0.7837(6)	0.7857(7)
$y$	0.4543(5)	0.4539(5)	0.4522(8)
$z$	0.3414(5)	0.3412(5)	0.3294(11)
O1 (3b) $x$	0.9238(10)	0.9239(10)	0.9289(19)
O2 (6c) $x$	0.4180(8)	0.4174(7)	0.4146(11)
$y$	0.7244(7)	0.7246(7)	0.7375(11)
$z$	0.1273(6)	0.1281(6)	0.1507(7)
O3 (6c) $x$	0.8779(10)	0.8786(10)	0.8832(14)
$y$	0.6951(10)	0.6941(10)	0.6947(14)
$z$	0.8153(11)	0.8139(10)	0.8197(14)
O4 (6c) $x$	0.8495(10)	0.8494(10)	0.8562(15)
$y$	0.6357(10)	0.6355(9)	0.6469(14)
$z$	0.1804(10)	0.1810(10)	0.1771(11)
O5 (6c) $x$	0.4760(9)	0.4753(11)	0.4832(12)
$y$	0.1464(8)	0.1470(8)	0.1423(12)
$z$	0.8453(10)	0.8444(10)	0.8299(18)
O6 (3b) $x$	0.1863(13)	0.1856(12)	0.1882(22)
O7 (6c) $x$	0.4717(7)	0.4726(7)	0.4842(13)
$y$	0.4652(9)	0.4654(8)	0.4572(13)
$z$	0.8181(10)	0.8134(10)	0.8123(11)
B1 (3b) $x$	0.3352(16)	0.3373(15)	0.3256(12)
B2 (6c) $x$	0.5536(11)	0.5559(10)	0.5517(9)
$y$	0.8806(10)	0.8818(9)	0.8824(13)
$z$	0.1498(8)	0.1525(9)	0.1685(15)
B3 (3b) $x$	0.7828(16)	0.7847(15)	0.7801(17)
Fe1-Fe1 (Å)	3.181(5)	3.177(4)	3.159(7)
Fe2-Fe2 (Å)	3.199(6)	3.195(6)	3.198(11)
2 x Dy-O3 (Å)	2.360(10)	2.372(10)	2.375(15)
2 x Dy-O4 (Å)	2.350(11)	2.352(10)	2.332(16)
2 x Dy-O7 (Å)	2.356(7)	2.347(6)	2.362(10)
$R_{Bragg}$	3.4	3.5	3.3
$R_{Mag}$	-	-	3.5

The high intensity temperature dependent data taken on D20 revealed the onset of additional magnetic scattering in the neutron diffraction patterns below about 40 K. Figure 1 shows for  $2\Theta < 70^\circ$  the thermal changes in the spectra in form of a difference thermodiffractogram where the data taken at 50 K were subtracted from all spectra. This eliminates the nuclear scattering and leaves only the purely magnetic scattering. All magnetic peaks appear at positions not corresponding to nuclear Bragg peaks and can be indexed using the magnetic propagation vector  $\tau = [0, 0, \frac{1}{2}]$ . The same propagation vector has been already found in all other  $R\text{Fe}_3(\text{BO}_3)_4$  compounds studied with neutrons [7-10]. It leads to a doubling of the magnetic unit cell in *c*-direction and is determined by the antiferromagnetic coupling between neighboring Fe spins along the helicoidal chain. The thermal dependence of the intensity of the different magnetic peaks seen in figure 1 is not identical (e.g. the  $(0 2 \frac{1}{2})$  reflection decreases on lowering the temperature) and indicates the presence of more than one magnetic sublattices having different temperature dependences. Magnetic symmetry analysis as implemented in the program BASIREPS which is part of the FULLPROF suite of programs [18, 19] was used to determine for  $\tau = [0, 0, \frac{1}{2}]$  the allowed irreducible representations and their basis vectors for the two possible magnetic sites (Fe and Dy) in  $P3_121$ . There are three allowed irreducible representations which were tested by refinement against the high resolution data taken at D2B at 3 K (figure 2b). It was found that only the basis vectors of one irreducible representation (IR) are describing the magnetic structure correctly. Table 2 lists the basis vectors of this IR and the refined values of their coefficients, the crystallographic details of the refinement are included in table 1.

**Table 2.** Basis vectors (BV) of the irreducible representation 3 for  $\tau = [0, 0, \frac{1}{2}]$  in  $P3_121$ . Refined values of their coefficients determined from the refinement of the magnetic structure of  $\text{DyFe}_3(\text{BO}_3)_4$  at 3 K. The coefficients describing the magnetic moment of Fe1 (BV2) and Fe2 (BV3) in *z*-direction were coupled.

	BV1	BV2	BV3
Fe1 (3b)			
$x, y, z$	1 -1 0	0 0 1	
$-y, x-y, z+1/3$	-1 -2 0	0 0 -1	
$-x+y, -x, z+2/3$	-2 -1 0	0 0 1	
Coefficient	0.09(14)	4.45(5)	
Fe2 (6c)			
$x, y, z$	1 0 0	0 1 0	0 0 1
$-y, x-y, z+1/3$	0 -1 0	1 1 0	0 0 -1
$-x+y, -x, z+2/3$	1 1 0	-1 0 0	0 0 -1
$y, x, -z$	0 1 0	1 0 0	0 0 -1
$x-y, -y, -z+2/3$	-1 0 0	1 1 0	0 0 1
$-x, -x+y, -z+1/3$	1 1 0	0 -1 0	0 0 1
Coefficient	0.00(1)	0.27(12)	-4.45(5)
Dy (3b)			
$x, y, z$	1 -1 0	0 0 1	
$-y, x-y, z+1/3$	-1 -2 0	0 0 -1	
$-x+y, -x, z+2/3$	-2 -1 0	0 0 1	
Coefficient	1.28(8)	-6.27(7)	

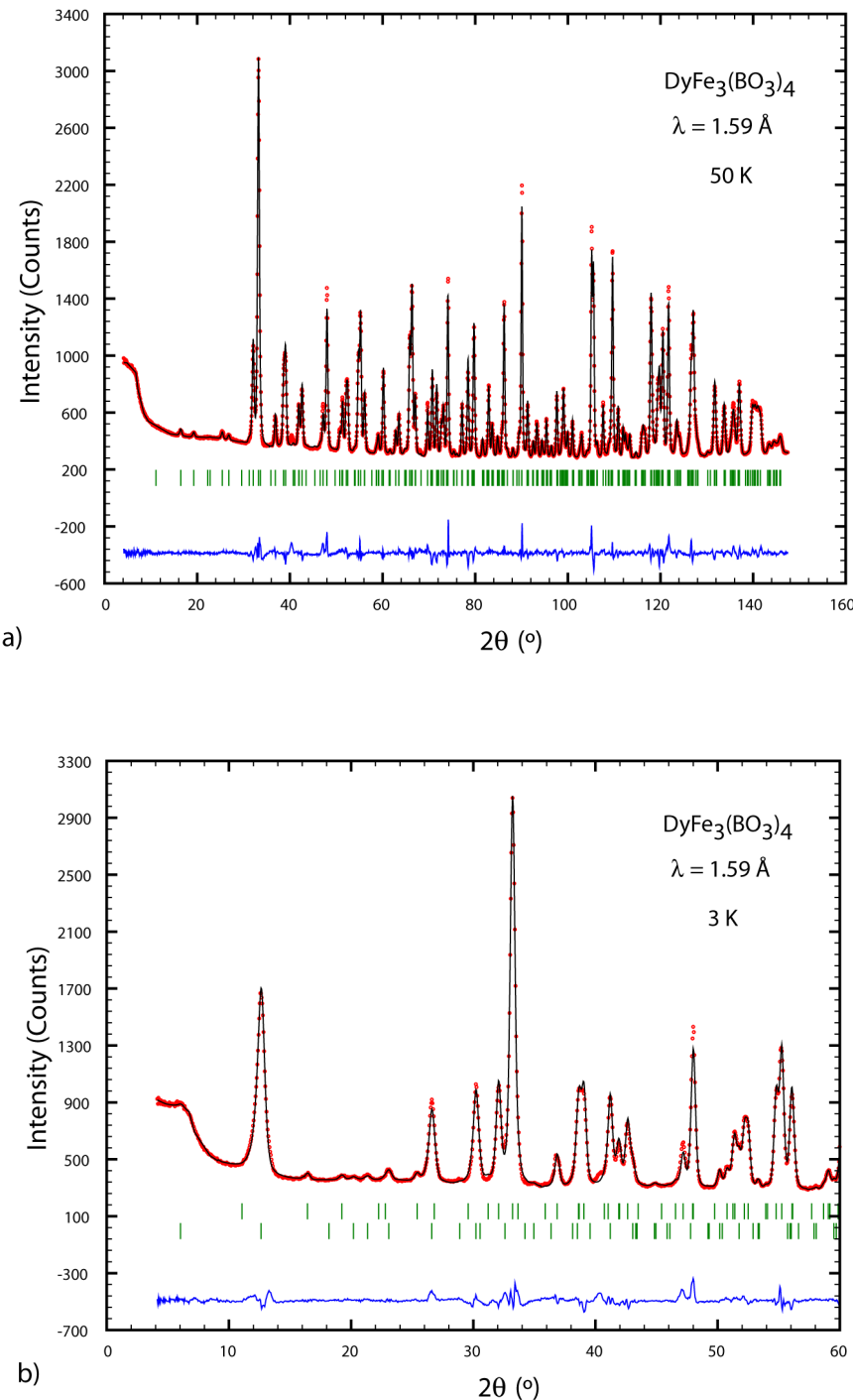


**Figure 2.** Observed (dots, red), calculated (line, black) and difference pattern of  $\text{DyFe}_3(\text{BO}_3)_4$  at a) 50 K in the paramagnetic state refined in  $P3_121$  and b) at 3 K in the magnetic state. The tick marks indicate the calculated position of the nuclear (upper row) and (for b)) magnetic (lower row) Bragg peaks.

The magnetic structure found (figure 3) resembles strongly those found for  $\text{TbFe}_3(\text{BO}_3)_4$  [7] and  $\text{PrFe}_3(\text{BO}_3)_4$  [8] with a dominant easy axis orientation of the magnetic moments. The coefficients of the basis vectors describing an easy plane orientation of the two iron sites are zero or very close to

zero (Table 2). Only the rare earth site sees a non negligible component within the hexagonal basis plane. As in the case of the easy axis compounds with  $R = Tb$  [7] and  $Ho$  (below 5 K) [9] the spins of the iron and the rare earth sublattice are aligned antiparallel within the hexagonal layers while the alignment had been shown to be parallel in the case of  $R = Pr$ . The different relative orientations of the two sublattices have been discussed in [8] and connected to the spin-orbit coupling of the rare earth. The magnetic moment value of iron amounts to about  $\mu_{Fe} = 4.5 \mu_B$  and corresponds to the values found in the other  $RFe_3(BO_3)_4$  compounds adopting the easy axis orientation approaching the value expected for a  $S = 5/2$  ion. The total magnetic moment of the  $Dy^{3+}$  ion is with  $\mu_{Dy} = 6.4 \mu_B$  largely inferior to the expected free ion value of  $10 \mu_B$ . The same situation had been found before in compounds with  $R = Ho$  ( $\mu_{Ho} = 5.1 \mu_B$ ) [9] and  $Er$  ( $\mu_{Er} = 5.1 \mu_B$ ) [8] but not in  $TbFe_3(BO_3)_4$  [7] where the ordered magnetic moment corresponds with  $\mu_{Tb} = 8.6 \mu_B$  nearly to the expected free ion value. The ordering of the rare earth sublattice is known to be induced first by the polarizing influence of the ordered Fe-sublattice before at lower temperatures indirect  $R-O-Fe-O-R$  or  $R-BO_3-R$  interactions start to play a role. One has to recall here that in the corresponding  $RA1_3(BO_3)_4$  compounds no long rang ordered magnetism exists [20]. Popova et al. [15] suggested from the interpretation of their magnetization data that the dysprosium subsystem in  $DyFe_3(BO_3)_4$  would stay essentially paramagnetic down to lowest temperatures. This has to be put into the context of the above discussed strong polarizing influence of the iron sublattice and our own neutron results: The ordering of the  $Dy$ -sublattice is not resulting from direct  $R-O-R$  exchange interactions but depending on the ordering of the Fe-sublattice, the value of the ordered magnetic moment  $\mu_{Dy} = 5.1 \mu_B$  is strongly reduced compared to the free ion value of  $Dy^{3+}$ , however, the neutron data clearly evidence the long range antiferromagnetically ordered nature of the  $Dy$ -sublattice. We would like to mention here the highly interesting results of Chaudhury et al. [21] who found in  $TmAl_3(BO_3)_4$  the existence of a large magnetoelectric effect generated in absence of any d-electron spins solely by the rare earth moment.

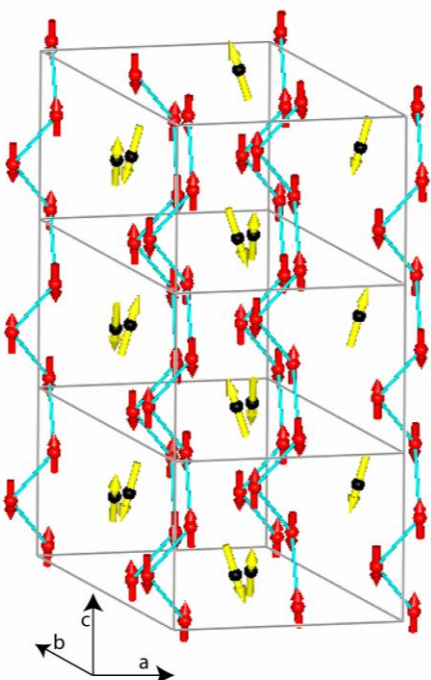


**Figure 3.** Magnetic structure of  $DyFe_3(BO_3)_4$ . Fe spins in red (black), Dy moments in yellow (light grey), the direct Fe-Fe exchange along the helicoidal chains is indicated by light blue (grey) lines.

In order to check for the presence of a possible spin reorientation (as found in  $\text{HoFe}_3(\text{BO}_3)_4$ ) and in order to verify whether both sublattices possess the same Néel temperature the temperature dependent high flux data of D20 were sequentially refined. For this refinement the atom coordinates were kept fixed at values determined from a fit of the high resolution data taken just above  $T_N$  at 50 K on D2B which presents purely nuclear scattering. Results of this refinement at 50 K are included in table 1 and show that the crystallographic structure does not undergo any significant changes between 50 K and 3 K validating the approach of fixing the atom coordinates for the sequential refinement. The refinement proceeded smoothly over the whole temperature range using the magnetic structure model found at 3 K. Figure 4 displays the temperature dependence of the total Dy moment, of the Fe moment and of the Dy basal plane component. It becomes clear that both sublattices start to get long range ordered at the same temperature,  $T_{\text{NDy}} = T_{\text{NFe}} = 38 K. No sign of a clear spin reorientation is found, one sees, however, that the basal plane component of the Dy sublattice is only present between 20 K and lowest temperatures. This coupling leads to a  $120^\circ$  arrangement of the Dy spins occupying the threefold Wyckoff site  $3b$  within a nuclear unit and has been already found as minority spin structure in  $\text{ErFe}_3(\text{BO}_3)_4$  [8]. It does not correspond to the simple collinear easy plane configuration as found in  $\text{HoFe}_3(\text{BO}_3)_4$  above 5 K [9] or in  $\text{ErFe}_3(\text{BO}_3)_4$  above 10 K [8]. Analyzing in more detail the temperature dependence of the total Dy moment increase (figure 5) one can notice that on lowering the temperature the moment increase is following the increase of the polarizing Fe sublattice magnetization. At about 25 K, however, one sees a reinforced increase and in parallel at about 20 K the arising of the basal plane component of the Dy moment. The basal plane component cannot be induced by the anisotropy of the Fe-sublattice as it does not - as explained before - correspond to the collinear easy plane arrangement, but has to be related to the symmetry of indirect R-R exchange interactions. This indicates, together with the accelerated total Dy-moment increase below 25 K, that the influence of the indirect R-R interactions becomes important at this relatively high temperature.$

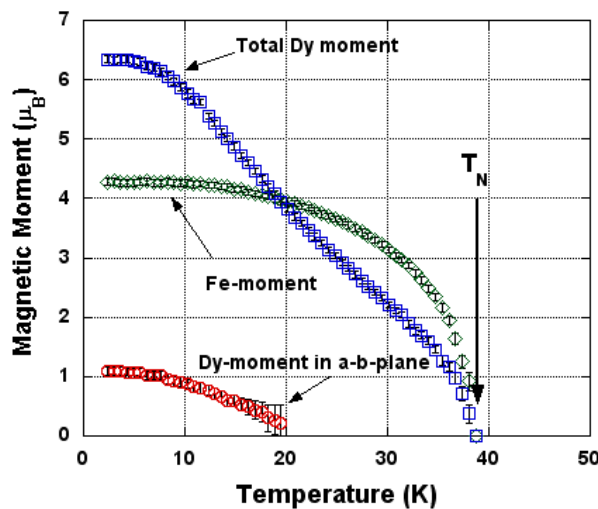


**Figure 4.** Temperature dependence of the magnetic moment values of the Fe-sublattice (diamonds), of the Dy-sublattice (squares) and of the basal plane component of the Dy-moment.

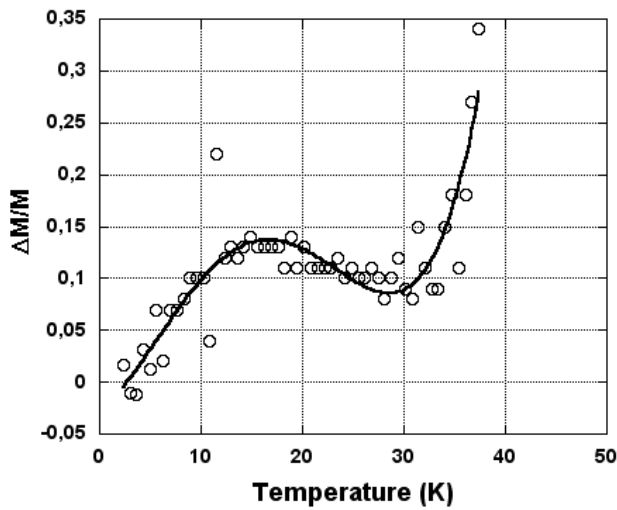


**Figure 5.** Temperature dependence of the Dy-moment increase.

Figure 6 displays the temperature dependence of the unit cell  $a$ -parameter where a small anomaly can be detected at about 27 K. This is the first evidence of such an thermal expansion anomaly in the family of  $RFe_3(BO_3)_4$  compounds. Its interpretation as a magnetostriction effect is not supported by our analysis of the temperature dependence of the sublattice magnetizations (figure 5). It can, however, be connected to the Schottky type anomalies seen in the susceptibility and specific heat data at about 23 K presented by Popova et al. [15] which were related to a repopulation of two low lying Kramers doublets. Changes in the anisotropy of the Dy-sublattice induced by this repopulation could eventually be as well responsible for the appearance at about 20 K of the basal plane magnetic moment component.

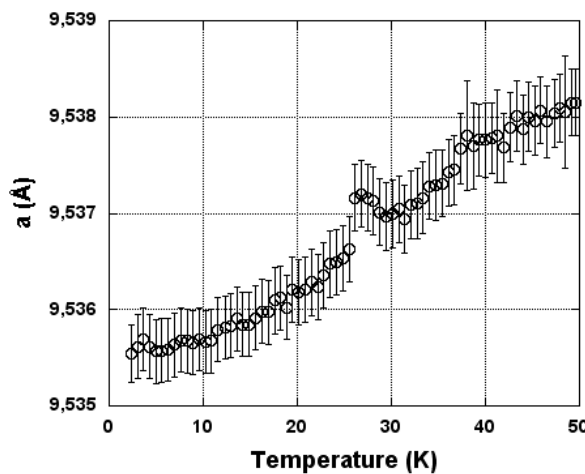


**Figure 6.** Temperature dependence of the unit cell  $a$ -parameter of  $DyFe_3(BO_3)_4$ .

#### 4. Summary

Temperature dependent neutron diffraction studies on  $DyFe_3(BO_3)_4$  show that this compounds magnetically orders at about  $T_N = 38$  K into a magnetic structure of predominantly easy axis type with

a magnetic propagation vector  $\tau = [0 \ 0 \ \frac{1}{2}]$ . Both magnetic sublattices order at the same temperature, magnetic moment values amount to  $\mu_{\text{Fe}} = 4.5 \ \mu_{\text{B}}$  and  $\mu_{\text{Dy}} = 6.4 \ \mu_{\text{B}}$ . A small magnetic component forming a  $120^\circ$  type arrangement of the Dy-spins appears below about 20 K. The appearance of this component and a small anomaly visible in the thermal expansion of the unit cell  $a$ -parameter at about 27 K might be connected to a repopulation of the lowest Dy<sup>3+</sup> energy levels.

### Acknowledgement

This work was supported by RFBR, grant no. 10-02-00765.

### References

- [1] Jaque D 2001 *J. Alloys Compounds* **323/324** 204
- [2] Chen X, Luo Z, Romero J J, Sole J G, Huang Y, Jiang A and Tu Ch 2001 *J. Phys.: Condens. Matter* **13** 1171
- [3] Kalashnicova A M, Pavlov V V, Pisarev R V, Bezmaternykh L N, Bayer M and Rasing Th 2004 *JETP Lett.* **80** 293
- [4] Zvezdin A K, Krotov S S, Kadomtseva A M, Vorob'ev G P, Popov Yu F, Pyatov A P, Bezmaternykh L N, Kuvardin A V and Popova E N 2005 *JETP Lett.* **81** 272
- [5] Zvezdin A K, Vorob'ev G P, Kadomtseva A M, Popov Yu F, Pyatakov A P, Bezmaternykh L N, Kuvardin A V and Popova E N 2006 *JETP Lett.* **83** 509
- [6] Campá J A, Cascales C, Gutiérrez-Puebla E, Monge M A, Rasines I and Ruiz-Valero C 1997 *Chem. Mater.* **9** 237
- [7] Ritter C, Balaev V, Vorotynov A, Petrakovskii G, Velikanov D, Temerov V and Gudim I 2007 *J. Phys.: Condens. Matter* **19** 196227
- [8] Ritter C, Vorotynov A, Pankrats A, Petrakovskii G, Temerov V, Gudim I and Szymczak R 2010 *J. Phys.: Condens. Matter* **22** 206002
- [9] Ritter C, Vorotynov A, Pankrats A, Petrakovskii G, Temerov V, Gudim I and Szymczak R 2008 *J. Phys.: Condens. Matter* **20** 365209
- [10] Fischer P, Pomjakushin V, Sheptyakov D, Keller L, Janoschek M, Roessli B, Schefer J, Petrakovskii G, Bezmaternykh L N, Temerov V and Velikanov D 2006 *J. Phys.: Condens. Matter* **18** 7975
- [11] Pankrats A, Petrakovskii G, Bezmaternykh L N and Bayukov O A 2004 *JETP* **99** 766
- [12] Hinatsu Y, Doi Y, Ito K, Wakeshima M and Alemi A 2003 *J. Solid State Chem.* **172** 438
- [13] Klimin S A, Fausti D, Meetsma A, Bezmaternykh L N, van Loosdrecht P H M and Palstra T T M 2005 *Acta Cryst. B* **61** 481
- [14] Rebbouh L, Desautels R D, Ritter C, Cadogan J M, Temerov V, Pankrats A and van Lierop J 2011 *Phys. Rev. B* **83** 140406(R)
- [15] Popova E A, Tristan N, Vasiliev A N, Temerov V L, Bezmaternykh L N, Leps N, Büchner B and Klingeler R 2008 *Eur. Phys. J. B* **62** 123
- [16] Gudim I A, Pankrats A I, Durnaikin E I, Petrakovskii G A, Bezmaternykh L N, Szymczak R and Baran M 2008 *Cryst. Rep.* **53** 1140
- [17] Volkov D V, Demidov A A and Kolmakova N P 2008 *JETP* **106** 723
- [18] Rodríguez-Carvajal J 1993 *Physica B* **192** 55  
<http://www.ill.eu/sites/fullprof/php/downloads.html>
- [19] Ritter C 2011 *Sol. St. Phenomena* **170** 263
- [20] Neogy D, Chattopadhyay K N, Chakrabarti P K, Sen H and Wanklyn B M 1996 *JMMM* **154** 127 and 1997 *J. Phys. Chem. Solids* **59** 783
- [21] Chaudhury R P, Lorenz B, Sun Y Y, Bezmaternykh L N, Temerov V L and Chu C W 2010 *Phys. Rev. B* **81** 220402(R)